A HW/SW Embedded System for Accelerating Diagnosis of Glaucoma From Eye Fundus Images

Paulo Cezar Dantas Junior
Centro de Informatica
Universidade Federal de Pernambuco
Recife, Brazil
paulo.cezar.gdj@gmail.com

Andrea Sarmento
Clinica Oftalmologica Zona Sul
Recife, Brazil
agsarmento@yahoo.com.br

Adriano Sarmento
Centro de Informatica
Universidade Federal de Pernambuco
Recife, Brazil
aams@cin.ufpe.br

ABSTRACT
Glaucoma is an irreversible eye disease in which the optic nerve is progressively damaged leading to blindness. However, it is manageable if diagnosed early. The most common screening exam for glaucoma diagnosis is the eye fundus evaluation in which the ophthalmologist examines the optic nerve and estimates the Vertical Cup to Disc Ratio (VCDR). Currently, VCDR evaluation is performed by ophthalmologists based on their visual perception and experience. This paper explores different embedded architectures based on low power processors and describes a HW/SW embedded system that automatically calculates VCDR from eye fundus images using image processing techniques. Optic disc diameter is calculated by a HW accelerator, while optic cup diameter is calculated by SW. This resulted in an embedded system that reduces at least 30% of the execution time of a SW-only implementation and that is significantly faster than other related works based on desktop computers. The proposed system was tested on 70 eye fundus images and achieved a 97.72% accuracy rate.

CCS Concepts
• **Computer systems organization→Embedded systems** • **Computing methodologies→Image segmentation.**

Keywords
HW/SW embedded system; Glaucoma; Architecture Exploration; HW acceleration; Image Processing.

1. INTRODUCTION
Glaucoma is an eye disease caused by elevated intraocular pressure in which the optic nerve is progressively damaged, leading to deterioration in vision and quality of life [1]. A research report published by British Journal of Ophthalmology predicted that a global toll of 80 million people would be affected by the disease by 2020 [2]. Unlike other eye diseases like cataract and myopia, glaucoma is not curable and vision loss cannot be repaired. Early detection is thus essential for early treatment to prevent vision deterioration and blindness [3].

RSP'16, October 06-07, 2016, Pittsburgh, PA, USA
© 2016 ACM. ISBN 978-1-4503-4535-4/16/10…$15.00
DOI: http://dx.doi.org/10.1145/2990299.2990303

The most common screening exam for glaucoma diagnosis is the eye fundus evaluation using an ophthalmoscope in which the ophthalmologist examines the optic nerve head (ONH). The ONH is the location where the optic nerve enters the back of the eye. In a typical eye fundus image, ONH has two distinguishable regions, an elliptical region called Optic Disc and a small bright region inside the optic disc which is called Optic Cup as illustrated in Figure 1. An important indicator of glaucoma is the Vertical Cup-to-Disc ratio (VCDR) defined as the ratio of the vertical height of the optic cup to the vertical height of the optic disc. Optic nerve damage (cupping) progresses as the cup becomes larger in comparison to the optic disc. VCDR values greater than 0.65 indicate high probability of glaucoma [4]. Currently, VCDR evaluation is performed by ophthalmologists based on their visual perception and experience.

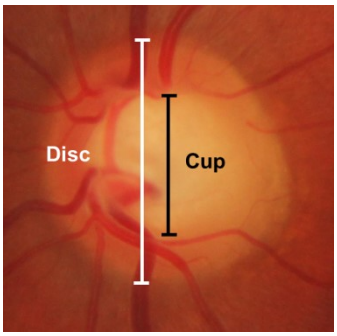

Figure 1 Optic Disc and Cup

Visual measurement of VCDR may reduce the accuracy of the exam, especially in developing countries or remote areas where there is a lack of properly trained professionals and proper equipment. In developing countries the lack of ophthalmologists results in less time to perform a full eye examination [5]. Most of the time, an ophthalmologist has less than five minutes not only to perform VCDR evaluation but also to look for other eye diseases such as diabetic retinopathy, age-related macular degeneration, etc. Therefore, accuracy and time spent on VCDR evaluation is important. Although there are systems such as OCT[20] (Optical Coherence Tomography) and HRT[21] (Heidelberg Retina Tomography) that can measure VCDR automatically, their high cost and the fact that they are not portable restrict their use in such countries or remote areas. There are existing works based on general computer systems that automatically calculate VCDR, but their high computational cost require great processing and

memory resources in order to provide a fast response. Additionally, there is no existing work that proposes an embedded system using low power processors that provides fast image processing and analysis of eye structures to deliver diagnosis of glaucoma.

This paper proposes a fast and low computational cost HW/SW embedded system for automatically classifying digital fundus image into either normal or glaucomatous types in order to aid ophthalmologists to give a more accurate diagnosis of glaucoma. Thus, the contributions of this work are: (1) a novel image processing method for calculating VCDR that requires less processing but is still accurate; (2) an extensive embedded system architecture exploration where different solutions with low power processors are proposed in order to provide a low cost architecture and (3) a HW/SW embedded architecture tailored to this application domain that accelerates the proposed VCDR calculation method providing very fast diagnosis. The proposed system was tested on 70 images of a public eye fundus image database and high accuracy diagnosis were provided in a few seconds which proves the efficacy of the proposed approach.

The rest of the paper is organized as follows: section 2 gives a short description of related works; section 3 explains the proposed VCDR evaluation method; section 4 explains how architecture exploration was performed in this work; section 5 details the proposed HW/SW architecture; section 6 presents experimental results and evaluates the proposed embedded system and section 7 draws some conclusions and future works.

2. RELATED WORKS

Some portable device based solutions for aiding the diagnosis or progression of glaucoma have been proposed. Portable Eye Examination Kit (Peek) [6] is a kit for acquiring eye images from a smartphone in order to simplify eye exams; however, it does not automatically calculates VCDR. The work proposed by [7] is a tablet app that performs visual field tests for evaluating visual loss due glaucoma progression.

Several general computer-based solutions using image processing techniques for VCDR estimation have been proposed in past works. Xu[8] employ a superpixel classification method for cup segmentation from an eye fundus image where the disc has already been segmented. Superpixels are segmented, blood vessels are extracted and removed, then superpixels are classified as part of the disc or cup based on color and location. Cheng [11] proposes another superpixel classification approach for disc and cup segmentation. Disc segmentation is performed by dividing the image in superpixels where some features of these superpixels are extracted and used for classifying superpixels as belonging or not to the optic disc; after that some morphological operations, Hough transform and an active contour model are applied to locate the disc center and detect the disc border. The process of cup segmentation is similar to disc segmentation.

Yin [9] presents a method that employs Canny edge detection, Hough transform, ellipse fitting algorithm, active contour model to segment the optic disc. Optic cup segmentation is almost identical, except that there is also a blood vessel removal and inpainting step.

Anusorn [10] uses morphological closing operation, Canny edge detection algorithm, K-means clustering algorithm and an ellipse fitting method for disc segmentation. For cup segmentation, histogram based on G channel is analyzed for defining a threshold in order to use a threshold level-set algorithm. After that morphological opening operation and an ellipse fitting algorithm are employed.

Liu[12] presents a level-set based approach for optic disc and cup segmentation. A level-set algorithm followed by an ellipse fitting method are employed for disc segmentation. Two different methods are used for cup segmentation: (1) the same level-set algorithm and ellipse fitting method; and (2) a color intensity based algorithm in which a point within the optic cup is first manually selected to get the characteristic color difference between the optic cup and surrounding optic disc region, and then the same ellipse fitting method is employed. Two kinds of results are generated which are fused by a neural network.

As can be seen most of the related works uses costly image processing methods, such as Hough transforms, Canny edge detection, K-means clustering and inpainting algorithms, being very processor intensive and memory consuming. Their focus is only on accuracy and they are intended to run in computer desktops that have great processing and memory capacity, not on an embedded system with strict processing and memory constraints.

3. VCDR EVALUATION METHOD

In order to identify glaucoma by VCDR evaluation, optic disc and cup have to be segmented. The proposed method flow is shown in Figure 2, where disc segmentation steps are shown on the left part and cup segmentation steps on the right. After disc and cup segmentation, VCDR evaluation is done. Vertical disc and cup diameters are calculated by getting the coordinates of the upper and lower pixels of disc and cup respectively. Then (1) is applied, where xlower, ylower and xupper, yupper are the x,y coordinates of the lower and upper pixels respectively. Finally, VCDR is defined as (2), where values greater than 0.65 indicates that a patient has high risk of having glaucoma.

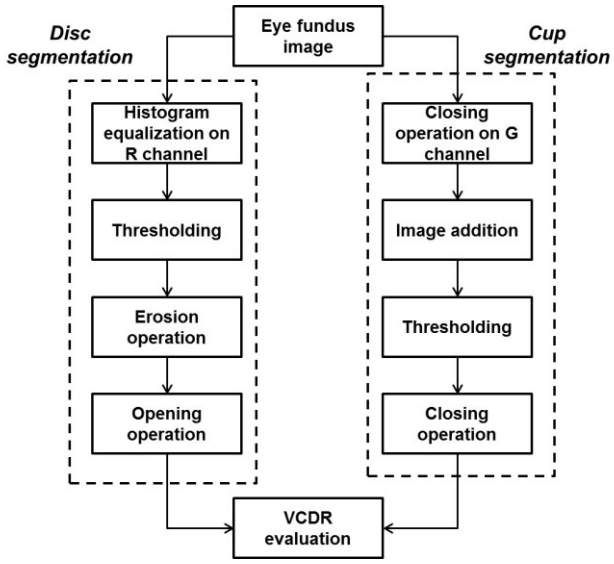

Figure 2 VCDR Evaluation Flow

$$d = \sqrt{(x_{lower} - x_{upper})^2 + (y_{lower} - y_{upper})^2} \quad \textbf{(1)}$$

$$VCDR = \frac{\text{Vertical Cup Diameter}}{\text{Vertical Disc Diameter}} \quad \textbf{(2)}$$

3.1 Disc Segmentation

In a RGB eye fundus image, the optic disc region has color intensity in the red (R) channel greater than others regions. Based on this analysis, disc segmentation uses only the red channel of the original image as shown in Figure 3(b). However, as the optic disc is a highly vascularized region and blood vessels also have a high intensity at the R channel, histogram equalization (Figure 3(c)) is applied to the R channel image to enhance contrast between disc and blood vessels.

The next step is applying threshold for isolating disc and removing blood vessels as illustrated in Figure 3(d). Threshold value was empirically set to 160, meaning that pixels values above or equal to 160 become white pixels and values below become black pixels.

Morphological erosion operation (Figure 3(e)) followed by a morphological opening operation (Figure 3 (f)) is performed to remove noises and to smooth disc edges. For erosion, a circular structuring element with 7x7 pixels is employed to remove (small) noise outside the disc region, while a circular structuring element with 11 x 11 pixels is applied for the opening operation smoothing disc border.

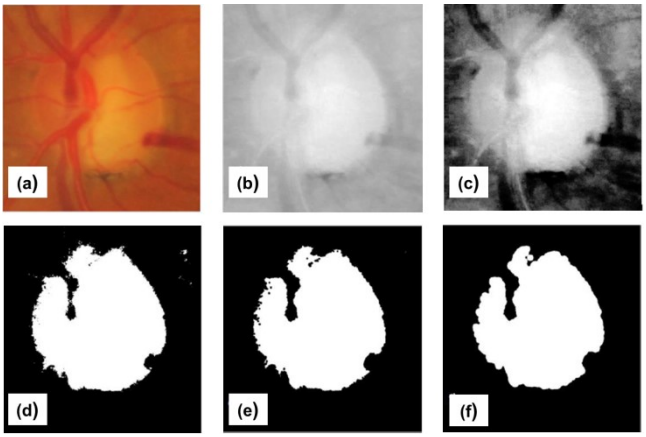

Figure 3 (a) Original image (b) Red channel image (c) Histogram equalization (d) Thresholding (e) Erosion (f) Opening

3.2 Cup Segmentation

Compared to optic disc extraction, cup segmentation represents an even greater challenge as the cup-disc boundary is usually less pronounced than that of the disc region. Moreover visibility is reduced as blood vessels intersect the cup-disc boundary.

As the green (G) channel of a fundus image presents higher contrast between cup and disc regions, cup segmentation only uses the G channel. Then a morphological closing operation with a circular structuring element generates a new image that is added to the G channel original image in order to improve the contrast between cup and disc. These two steps result in an image similar to Figure 4(b).

After that, thresholding is done to remove blood vessels as shown in Figure 4(c). Threshold value was empirically set to 255. The last step is employing a closing operation using a circular structuring element with 11x11 pixels to fill existing holes as illustrated on Figure 4(d).

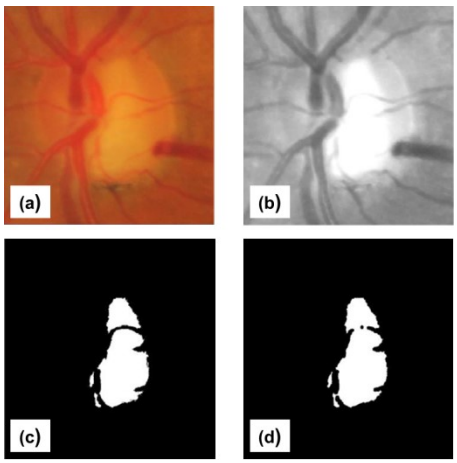

Figure 4 (a) Original image (b) Green channel image after closing and adding (c) Thresholding (d) Closing

The size and form of structuring elements have a great impact not only on the effectiveness of the method, but also on computational cost. Morphological operations can be very computer intensive. On the proposed approach, structuring elements were defined empirically based on minimizing processing time and memory consumption. Moreover, some regions (such as upper and lower borders) of the image do not have to be compared to structuring elements, as optic disc and cup are near the center of the image.

While the proposed approach uses morphological operations similar to other related works, it avoids more costly additional steps. In this work, additional steps such as histogram equalization and thresholding are linear in space and time (O(n)). Most of the related works use costly techniques such as Hough transform, Canny edge detection and K-means clustering that have computational complexity, respectively, of $O(n^3)$, O(n log n) and O(n log n). Additionally, the proposed algorithm does not need to employ any ellipse fitting method, as only the vertical diameter is analyzed.

4. EMBEDDED SYSTEM ARCHITECTURE EXPLORATION

The proposed VCDR evaluation method was implemented using a SW-only approach and a HW/SW approach. For the SW-only approach, different ways of implementing the proposed method and different low power processors were evaluated.

SW was first implemented sequentially where disc segmentation was followed by cup segmentation. And then SW was implemented concurrently as disc and cup segmentation flows have independent paths. The next step was evaluating SW execution time in 3 different low power processors: ARM1176JZF-S, ARM Cortex-8 and Intel Atom. Finally, performance analysis was performed on the SW-only implementation to identify possible bottlenecks.

After performance analysis, we started gradually to move some consuming time operations (especially those related to disc segmentation) to HW. After that, we analyzed communication cost, because communication could represent a bottleneck. Communication cost includes device driver execution time, data transfer time and communication protocol overhead. We had a HW/SW prototyping board in which communication is done through PCI and Avalon buses as explained in the next section. So

we estimated buses transfer times (including execution time of some parts of the device driver) based on a previous work [16]. As a result, a HW/SW architecture was defined in order to reduce execution time.

5. HARDWARE/SOFTWARE EMBEDDED SYSTEM

This approach proposes a HW/SW embedded system to perform VCDR evaluation, where most of disc segmentation is implemented by a HW accelerator while cup segmentation and VCDR evaluation are implemented by an embedded processor.

5.1 Hardware/Software Architecture

The HW/SW partitioning of the system is shown in Figure 5. SW reads the eye fundus image and performs histogram equalization on it before sending this new image to the HW module responsible for disc segmentation. While HW performs disc segmentation, SW can proceed to cup segmentation and cup diameter estimation. After HW finishes, SW can estimate disc diameter and finally evaluate VCDR.

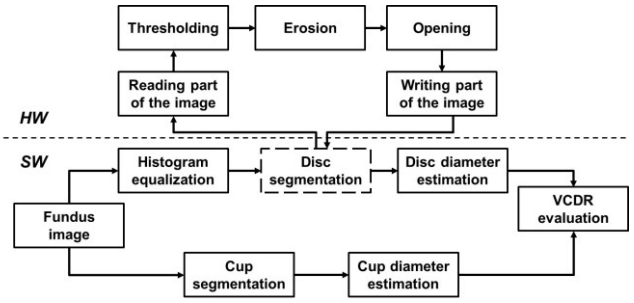

Figure 5 HW/SW Partitioning

Partitioning was based on analysis of processing time and the type of computation required in each step of the algorithm. Another aspect taken into account was minimizing communication time. The morphologic operations of the disc segmentation step took more time to execute compared to the ones used in cup segmentation, so these operations were moved to HW. However, disc and cup diameter estimation and VCDR calculation require floating point operations, thus these steps were implemented in SW as usually processors provide fast floating point units. Histogram equalization was also left to SW because, on the HW size, memory size was restricted and the whole image is required in order to perform this step. Moreover, communication time is reduced by performing histogram equalization on the SW side, as the result of this step is an R channel image, which is smaller than the original image.

The embedded system was implemented on a platform that has an Intel Atom 1.6GHz processor and an Altera Cyclone IV GX FPGA. The proposed HW/SW architecture is illustrated in Figure 6. SW communicates to HW through a PCI Express bus at a 125 MHz frequency using a PCI Express (PCIex) driver. The HW Disc segmentation module is connected to an Avalon bus [13] at 50 MHz frequency. There is a PCIex/Avalon adapter for translating PCIex requests in Avalon requests, enabling HW/SW communication. SW sends commands and image through the PCIex driver. HW receives commands through two parallel I/O ports, while the image is stored in a shared 810 KB dual port on-chip memory on the FPGA.

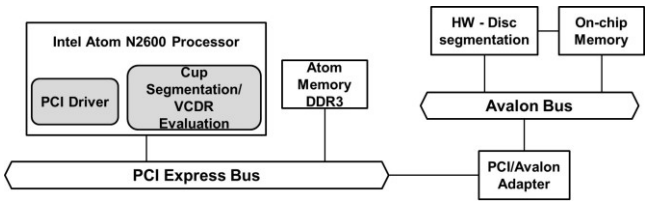

Figure 6 HW/SW Architecture

5.2 Hardware/Software Implementation

The SW part was implemented in C language not using any special image processing library. CentOS[14] which is a Linux distribution compatible to Red Hat was used as the operating system. HW was written in Verilog and generated by Altera Quartus and Qsys system integration tools [15].

Figure 7 shows the HW/SW implementation flowchart, where most of what the PCIex SW driver does is depicted. SW sends images to HW through the shared on-chip memory. Images sent to HW have only the R channel, meaning that each pixel is represented by a single byte. As the shared memory size is restricted, SW does not store the whole image in memory. It keeps sending parts of the image in a loop, storing 11 rows of pixels in each iteration. SW sends 11 rows because the morphological opening operation on the HW side uses an 11x 11 structuring element. This means that in order to process a single line, HW requires 5 rows above and 5 rows below the processed row. Then SW keeps doing that until HW processes the whole image. Notice that each time SW sends 11 rows of the image, these rows overwrite the previous 11 rows that were stored in the shared memory.

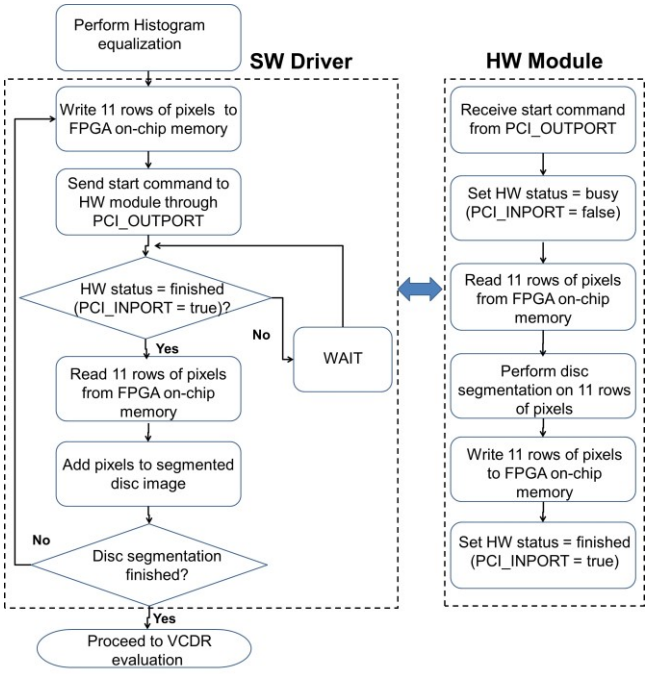

Figure 7 HW/SW Implementation Flowchart

The PCIEx SW driver provides two communication primitives for reading/writing from/to memory (pci_mm_read and pci_mm_write) and two communication primitives for sending

commands and receiving status to/from HW (pci_send_command and pci_get_status). PCIex driver communicates to HW through on-chip memory dual port and two parallel I/O ports: PCI_OUTPORT and PCI_INPORT. Data is sent to memory and the driver sends a start command to HW through the PCI_OUTPORT. On the HW side as soon as it receives the start command, it begins reading 11 rows of the image and processing one line of the image. Then when HW finishes, HW stores the processed row in the shared memory and sets the status signal sending it to the PCIe driver through the PCI_INPORT. PCIex driver reads PCI_INPORT and sends more data. SW uses Linux mmap function to map the physical address of the PCIex bus to a user-space pointer so it can be used in the C program as a regular pointer. Physical addresses of the PCIex bus, the parallel I/O ports and shared memory ports are obtained by Qsys tool.

For accelerating disc segmentation, the HW disc segmentation module does not have to process the first and the last five rows of the equalized image. As optic disc is near the center of the image, the rows near the top and bottom of the image can be neglected. So the first row of pixels that is generated by HW is actually the sixth row of the segmented image. Still, SW needs to send these first five rows because HW requires five rows above and below to process the sixth row.

6. EXPERIMENTAL RESULTS AND ANALYSIS

For validating the proposed VCDR calculation method, 70 low resolution fundus images were evaluated. 44 images were from healthy patients and 26 were from glaucomatous ones. Fundus images were obtained from RIM-ONE public image database [17]. RIM-ONE has images acquired from different hospitals, meaning that they were taken from different digital cameras with different resolution. RIM-ONE has different releases and in this work the first release was employed as a training set to adjust thresholding values (using 30 images), while the second release was used as experimental set (using different images). Image size is variable as experiments were performed on images acquired from different cameras. On average, images size is 700x700 pixels. All images were evaluated by ophthalmologists providing a gold standard.

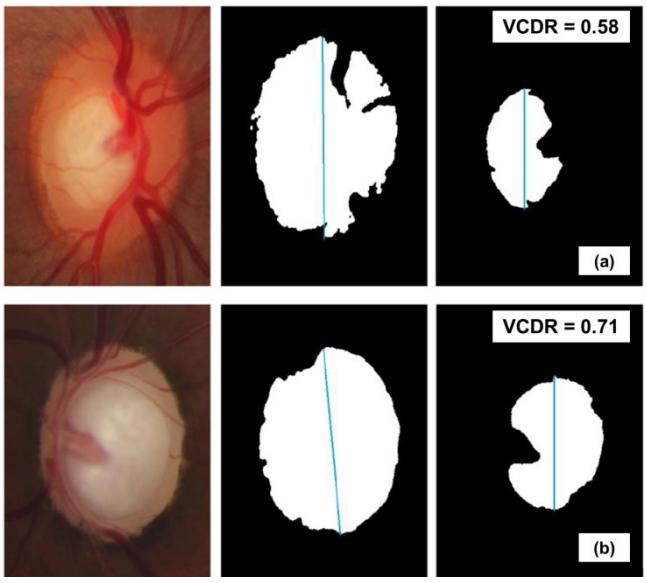

Figure 8 (a) VCDR evaluation from healthy patient, (b) VCDR Evaluation from glaucomatous patient

Figure 8 shows the results of the proposed VCDR evaluation method on two eye fundus images of RIM-ONE database. The first one (Figure 8(a)) is from a healthy patient (VCDR <= 0.65), while the second one (Figure 8(b)) is from a glaucomatous patient (VCDR > 0.65).

Table 1 shows the results of the proposed VCDR evaluation method concerning accuracy. This VCDR evaluation method made a correct diagnosis in 68 out of 70 images which gives an overall 97.72% accuracy rate. The proposed algorithm was evaluated using images captured from different cameras and still provided high accuracy. Meaning that the proposed algorithm could likely be integrated to works that deal with image acquisition such as Peek[6].

Table 1 Accuracy Evaluation

	Number of Images	Correct Evaluation	% of Accuracy
Healthy Patient	44	42	95.45
Glaucomatous	26	26	100.00
Overall	70	68	**97.72**

Comparison between this approach and other related works is presented in Table 2. Although these works use different image sets (related works used local image databases), it is fair enough to compare them. All of them use low resolution images as this work. As the approach of Xu[8] does not provide the same accuracy metrics, its accuracy value was left out. Notice that the proposed approach provides an accuracy rate better than other related works, which proves the efficacy of this approach.

Table 2 Accuracy Comparison to Related Works

	% of Accuracy
Yin[9]	91.00
Anusorn[10]	89.00
Cheng[11]	90.80
Liu[12]	91.50
This approach	**97.72**

One goal of this work is accelerating glaucoma diagnosis, so performance was also evaluated. Performance was evaluated comparing execution time of the proposed HW/SW approach to related work, as well as SW-only solutions of the proposed VCDR evaluation method. Yin[9] does not provide execution time but as his work use costly image processing techniques such as Hough transform, it is reasonable to presume that execution time is higher than our proposed approach. In general, the related works do not provide information about the employed programming language or operating system. These aspects may certainly impact execution time. In this work, comparison was based on the type of processor and amount of memory used on these related works.

Xu[8] runs a cup segmentation method on a 3.4 GHz quad-core processor with 12 GB DRAM. Anusorn[10] provides only disc segmentation execution time that is run on a 3 GHz dual-core processor (no information about memory is provided). Cheng[11] runs a VCDR calculation method on a 3 GHz dual-core processor with 3.25GB DRAM. And Liu[12] runs a VCDR calculation method on an Intel Xeon 2.4 GHz dual-core processor with 4 GB DRAM.

In experiments, the proposed approach was implemented on four different platforms: (1) Raspberry PI Model B[19] that has an ARM1176JZF-S 700MHz processor with 512 MB DRAM and running Raspbian 3.18 operating system; (2) Beagleboard-xM [18] that has an ARM Cortex-A8 1GHz processor with 512 MB DRAM running Ubuntu 14.04.2 operating system; (3) Intel Atom processor with 2GB DRAM; and (3) the proposed HW/SW architecture with Intel Atom and FPGA. Table 3 shows the results.

Table 3 Performance Analysis

	Platform Details	**Execution Time (seconds)**
Xu[8] (only cup segmentation)	3.4 GHz quad-core, 12 GB DRAM	20.2
Anusorn (only disc segmentation)	3.0 GHz dual-core	10.0
Cheng	3.0 GHz dual-core, 3.25 GB DRAM	13.5
Liu	Intel Xeon 2.4 GHz quad-core, 4 GB DRAM	7.4
Proposed Approach		
Raspberry-PI Model B	ARM1176JZF-S 700MHz, 512 MB DRAM	17.0
Beagleboard-XM -	ARM Cortex-A8 1GHz, 512 MB DRAM	10.3
Intel Atom	Intel Atom 1.6 GHz, 2GB DRAM	6.1
HW/SW	Intel Atom, 2GB Altera Cyclone IV GX FPGA, 810KB on-chip memory	**4.2**

As can be seen in Table 3, the proposed VCDR evaluation method outperforms most of related works when executed on three different platforms (Beagleboard, Intel Atom only, HW/SW). The only exception is the work of Liu[12] that is faster than the Beagleboard implementation. However, Liu uses a platform that has much more processing and memory resources. Results show that Intel Atom-only solution reduces execution time in 20% when compared to Liu approach. This solution is also more than 2 times faster than the other related works. These results are even more impressive because the processing and memory resources used on the related works are significantly greater than the ones used on those four platforms. Related works were implemented to run typically on a computer desktop, while the proposed approach is able to run on an embedded system with restricting processing and memory resources. The proposed VCDR evaluation method was executed on low power processors such as ARM Cortex-8, ARM1176JZF-S and Intel Atom commonly used on embedded systems, with less memory resources.

The proposed HW/SW implementation has the smallest execution time. HW/SW implementation provides 44%, 75%, 59% and 30% execution time reduction when compared to Liu's[12], ARM1176JZF-S, ARM Cortex-8 and Intel Atom-only solutions, respectively. While this result shows the advantage of adopting a HW/SW approach, it is clear that execution time could have been reduced even more. The main reason for not reducing more significantly execution time is due the limitation imposed by FPGA's on-chip memory. This resulted in an important communication overhead because SW could only send 11 pixels rows at a time and as a consequence there is a significant delay by the multiple calls of the SW communication layer. However, this may be easily fixed by using for example a DMA controller.

Although reducing execution time in some seconds may not seem so significant for this kind of application, this is very important for developing countries where the lack of ophthalmologists results in a very constraint time to perform a full examination as the number of patients is very large. The proposed system not only may reduce diagnosis errors but also allow ophthalmologists to spend more time examining other diseases or examining more patients.

Another important aspect is that the proposed system is implemented using low power processors which ease its use in low cost portable devices. Low cost and portability are mandatory characteristics for adopting such kind of system in developing countries or remote areas.

This work does not deal with image acquisition yet. However, the HW/SW platform used in this work allows the integration of a camera module (TRDB-D5M 5 Megapixels camera). Actually, this camera was used on a previous work [16], so camera integration will not be a complex task to do. Even though, image acquisition increases execution time, the proposed algorithm might be simplified as all images are captured from the same camera with fixed settings. For instance, the histogram equalization step to enhance contrast may be suppressed, reducing execution time even more.

7. CONCLUSIONS AND FUTURE WORKS

Early glaucoma diagnosis is essential for early treatment to prevent vision deterioration and blindness. The subjectivity related to a visual measurement of VCDR may reduce the accuracy of glaucoma evaluation, especially in developing countries or remote areas where there is a lack of properly trained professionals and proper equipment.

This work presents a HW/SW embedded system that implements a novel VCDR evaluation method to automatically diagnose glaucoma. The main benefit of this VCDR evaluation method is having low computational cost while maintaining accuracy comparable to other related works. Results showed that this method can be implemented on low power embedded processors and still reduce execution time and be accurate. The proposed HW/SW architecture is capable of reducing execution time in at least 30% which proves the efficacy of the approach.

Future works include integrating the TRDB-D5M digital camera in the HW/SW platform in order to implement a full embedded system that provides image acquisition and glaucoma diagnosis. This may simplify the proposed algorithm and enable further improvements on execution time. Further architecture exploration will also be done. Different HW/SW communication schemes such as introducing DMA controllers to manage image transfers

from the processor to the HW accelerator module will be explored in order to reduce communication overhead. Other aspect that will be addressed is developing cheaper and energy efficient solutions by using different embedded processors such as ARM processors in the HW/SW architecture as this system is intended to be adopted in developing countries and remote areas. In this context, not only performance will be evaluated but also processor cost and energy consumption. Finally, another type of image processing accelerator may be explored such as GPUs, for instance Raspberry PI boards have simple GPUs on it.

8. REFERENCES

[1] Kass, M.A., Heuer, D.K., Higginbotham E.J., Johnson, C.A., Keltner, J.L., Miller, J.P., Parrish, R.K., Wilson, M.R., Gordon, M.O. 2002. *The Ocular Hypertension Treatment Study: a randomized trial determines that topical ocular hypotensive medication delays or prevents the onset of primary open-angle glaucoma*. Arch Ophthalmol; 120:701–13; discussion 829–30J, 2002.

[2] Quigley, H.A., Broman, A.T. *The number of people with glaucoma worldwide in 2010 and 2020*. British J. Ophthalmology 90, 262–267, 2006.

[3] Rylander, N.R., Vold, S. D. 2008. *Cost analysis of glaucoma medications*. Am J Ophthalmol, vol. 145, pp. 106-13, Jan 2008.

[4] *CE Lesson: 2014*. http://cms.revoptom.com/print.asp?page=osc/3146/lesson.htm.. Accessed: 2014- 12- 01.

[5] Resnikoff, S., Felch, W., Gauthier, T.M., Spivey, B. 2012. The Number of Ophthalmologists in Practice and Training Worldwide: A Growing Gap Despite More than 200000 Practitioners. British Journal of Ophthalmology , March 2012.

[6] *Peek – Professional Eye Examination Kit*. http://www.peekvision.org/. Acessed 2015-09-01P.

[7] *Tablet screening app can improve eye health outcomes in remote, underserved communities*. News Medical-Life Sciences & Medicine. http://www.news-medical.net/news/20141021/Tablet-screening-app-can-improve-eye-health-outcomes-in-remote-underserved-communities.aspx . Accessed: 2015-09-01.

[8] Xu, Y., Liu, J., Lin, S., Xu, D., Cheung, C., Aung, T., Wong, T., *Efficient Optic Cup Detection from Intra-image Learning with Retinal Structure Priors*. In 15th International Conference on Medical Image Computing and Computer-Assisted Intervention, MICCAI 2012, pp.58–65, Nice, 2012.

[9] Yin, F., Liu, J., Wong, D., Tan, N., Cheung, C., Baskaran, M., Aung, T. and Wong, T. Automated segmentation of optic disc and optic cup in fundus images for glaucoma diagnosis. 25th IEEE International Symposium on Computer-Based Medical Systems (CBMS), 2012.

[10] Anusorn, C.B., Kongprawechon, W., Kondo, T., Sintuwong, S. 2013. Image processing Techniques for glaucoma detection using the cup to disc ratio. Thammasat International Journal of Science and Technology, March 2013.

[11] Cheng, J., Liu, J., Xu, Y., Yin, F., Wong, D., Tan, N., Cheng, C., Aung, T. and Wong, T. *Superpixel classification based optic disc and optic cup segmentation for glaucoma screening. Medical Imaging*, IEEE Transactions on, vol. 32, no. 6, pp. 1019—1032, 2013

[12] Liu, J., Yin, F. S., Wong, D. W., Zhang, Z., Tan, N. M., Cheung, C. Y., Baskaran, M., Aung, T., Wong, T. Y.. Automatic glaucoma diagnosis from fundus image. In IEEE 33rd International Conference of Engineering in Medicine and Biology Society (EMBS), 2011

[13] Altera. *Avalon Interface Specifications*. https://www.altera.com/content/dam/altera-www/global/en_US/pdfs/literature/manual/mnl_avalon_spec.pdf. Acessed 2015-09-01

[14] CentOS Project. https://www.centos.org/. Acessed 2015-09-01.

[15] Altera. *Qsys – Altera's System Integration Tool*. https://www.altera.com/products/design-software/fpga-design/quartus-prime/quartus-ii-subscription-edition/qts-qsys.tablet.html . Acessed 2015-09-01

[16] Souza, L., Oliveira Junior, L., Rios, M. *Development of a Portable Electronic Device to Assist the Diagnosis of Open Angle Glaucoma*. Intel Embedded System Contest 2014, http://sbesc.lisha.ufsc.br/sbesc2014/accepted_works. Acessed 2015-09-01.

[17] Fumero, F., Alayon, S., Sanchez, J.L., Sigut, J., Gonzalez-Hernandez, M. 2011. RIM-ONE: An Open Retinal Image Database for Optic Nerve Evaluation". In 24th International Symposium on Computer-Based Medical Systems (CBMS), June, 2011.

[18] Beagleboard, *Beagleboard-xM*, http://beagleboard.org/beagleboard-xm. Acessed 2015-09-01

[19] Raspberry. *Raspberry PI Model*. https://www.raspberrypi.org/products/model-b. Acessed:2015-12-01

[20] Kiersten, B., *What Is Optical Coherence Tomography?* American Academy of Ophthalmology, http://www.aao.org/eye-health/treatments/what-is-optical-coherence-tomography. Acessed 2015-12-01

[21] Heidelberg Engineering, *HRT Glaucoma Module* http://www.heidelbergengineering.com/international/products/hrt/hrt-glaucoma. Acessed: 2015-12-01.